

Subpicosecond dynamics of excitons and photoexcited intrinsic polarons in the quasi-one-dimensional solid PtCl

G. S. Kanner, G. F. Strouse, and B. I. Swanson

Materials Science and Chemical Science and Technology Divisions, MS G755, Los Alamos National Laboratory, Los Alamos, New Mexico 87545

M. Sinclair

Department 1812, MS1405, Sandia National Laboratories, Albuquerque, New Mexico 87185

J. P. Jiang and N. Peyghambarian

Optical Sciences Center, University of Arizona, Tucson, Arizona 85721

(Received 20 September 1996; revised manuscript received 18 February 1997)

Subpicosecond transient absorption (TA) spectroscopy was used to identify excited states, and to measure their relaxation kinetics as a function of excitation wavelength in the halogen-bridged transition-metal (MX) compound PtCl. For pump photon energies E_{pump} between 1.3 and 1.8 eV, below the threshold for exciton formation, intrinsic polarons are photoexcited and decay within 1–3 ps. Excitation into the exciton absorption tail (2.0–2.3 eV) yields singlet excitons that rapidly decay into an even-parity state, which has a lifetime (~ 100 ps) varying with the initial photon energy. Excitation (3.1 eV) well above the exciton threshold appears to generate more slowly decaying excitons, as well as polarons that are formed upon exciton dissociation. The TA spectra also indicate that relaxation of excitons for $E_{\text{pump}} > 2$ eV is mediated by large-amplitude vibrations perpendicular to the chains. Using third-harmonic generation spectroscopy in addition to TA, we develop an energy-level diagram for the excited states, including polaron levels, and the lowest odd- and even-parity excitons. [S0163-1829(97)02526-5]

I. INTRODUCTION

The halogen-bridged transition-metal (MX) compounds are of interest from a fundamental point of view because they exhibit a wide variety of broken-symmetry ground states and excited electronic states that are unique to one-dimensional (1D) systems.¹ The ground state, for example, can be tuned chemically, from a strong charge-density wave (CDW) with large lattice distortion (PtCl), to a weak CDW with small distortion (PtI), to an undistorted magnetic state (NiBr). Thus, MX solids provide a convenient means for studying competing electron-electron and electron-phonon interactions, which may help elucidate the behavior of more complex higher-dimensional systems. For example, a close analogy exists between the electronic properties of MX chains and those of CuO planes of high-temperature superconductors.² From a practical standpoint, these materials serve as models for the active semiconductors in devices such as light-emitting diodes and solar cells because of their remarkable tunability in the bandgap upon chemical substitution¹ or hydrostatic pressure.³ In contrast with conducting polymers, another class of 1D systems, MX solids grow as single crystals with primarily intrinsic disorder associated with zero-point motion and thermal fluctuations.⁴

The excited electronic states of 1D compounds have traditionally been described by semiconductor band models.^{5,6} Recently, however, there has been growing experimental evidence that excitations in conducting polymers more closely resemble those of their molecular analogs, the finite polyenes.⁷ The electronic states can be described as excitonic bands, with symmetries reflecting the C_{2h} point group of the

polymer chains. Similarly, for PtCl, in which excitations are very localized,⁶ both experiments⁸ and theory⁹ indicate that an excitonic rather than band picture is more appropriate. The lowest energy odd-parity exciton $|1u\rangle$ has a threshold at 10 K of 2.4 eV,⁴ and is associated with the transfer of an electron from the Pt^{2+} band to the Pt^{4+} band. Above the exciton band is another broad feature $|2u\rangle$, with a threshold of about 3 eV, which can be ascribed to either a continuum, a higher-energy exciton or a transition across the chains. Electroabsorption⁸ and third-harmonic generation (THG) measurements¹⁰ suggest the presence of an even-parity exciton $|mg\rangle$ in the energy range between 3.4 and 3.8 eV. The results of steady-state photoinduced absorption, photoinduced Raman spectroscopy, and light-induced electron paramagnetic resonance measurements have been interpreted within a band model in terms of the existence of nonlinear localized excited states associated with the 1D nature of MX systems, such as solitons and polarons.¹¹ These states can either exist as intrinsic defects in the materials, or are generated by photons of energy greater than the optical gap. Transient absorption data have also been explained by the simultaneous photogeneration of self-trapped excitons and polarons.¹² In all of the above cases, the photon energy of the exciting light (E_{pump}) exceeded the optical gap of the sample, and was therefore expected to give rise primarily to excitonic species. For lower E_{pump} , disorder plays an important role. In conducting polymers, for instance, the typically broad distribution of conjugation lengths may be the main contribution to the tail of the absorption spectrum. Consequently, it has been suggested that as the excitation energy is lowered within the tail, excitons of greater spatial extent are

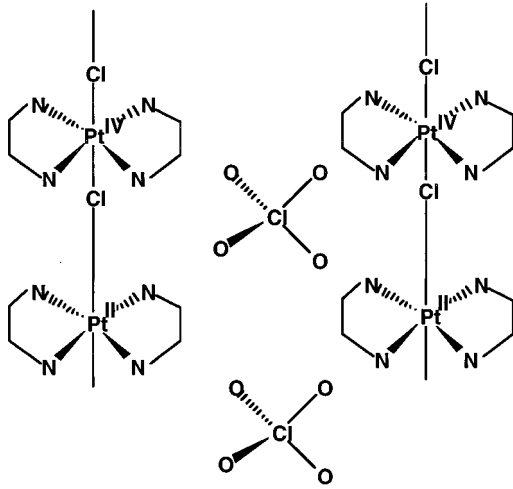


FIG. 1. Structure of the MX compound $PtCl$, showing sections of two adjacent chains with perchlorate counterions between them.

formed. The more tightly bound excitons created with higher-energy photons, however, decay faster presumably because of the larger number of accessible states to which they can hop, as revealed by transient luminescence and absorption measurements in poly(paraphenylenevinylene) (PPV).¹³ The situation in ordered MX solids is different because of the lack of structural inhomogeneity.⁴ Instead of generating excitons, subgap excitation may give rise primarily to excited states of species that already exist as intrinsic defects, such as electron (P^-) and hole (P^+) polarons, which are correlated with a subgap “A” band at 1.65 eV in the linear absorption of $PtCl$.^{14,15}

It is the purpose of this work to identify excited states and their relaxation dynamics as a function of excitation into three regions of the linear absorption—below, within, and above $|1u\rangle$ —and to understand the nature of intrinsic versus extrinsic disorder, which characterizes photoexcited states in ordered MX solids and typical conducting polymers, respectively. In this work we describe experiments on the strongly localized MX compound $[Pt(en)_2][Pt(en)_2Cl_2] \cdot (ClO_4)_4$ (Fig. 1), where (en) represents ethylenediamine; we shall refer to this solid as $PtCl$.

II. EXPERIMENT

A Coherent Mira Ti sapphire laser with 200 fs pulses at 800 nm and 76 MHz repetition rate was used to seed a Quantronix optical amplifier, producing 250 fs pulses each of 500 μJ at 1 kHz. These pulses then produced a white light continuum in a cell of flowing water. About 5% of this light was used for a probe beam, the rest, time-delayed and then spectrally narrowed with a 10 nm bandwidth interference filter for wavelengths from 550 to 900 nm; this portion constituted the pump. For measurements with excitation at 400 nm, we frequency-doubled part of the amplifier output in a 200 μm thick BBO crystal. A different $PtCl$ crystal was used for each E_{pump} to exclude effects due to the excitation wavelength dependence of long-lived defect states.¹⁶

A 298×1152 pixel Princeton Instruments CCD coupled to a 0.15 m Acton spectrometer was used for detection of the

photoinduced changes in transmission $-\Delta T/T$ of the probe in the spectral range from 1.2 to 4.0 eV. However, since the samples of $PtCl$ were relatively thick (60–300 μm), it was not possible to detect the transmission of probe light polarized parallel to the chains for photon energies above 2.2 eV. Transmission measurements through a $PtCl$ plate were also performed as a function of laser intensity using a Si photodiode and an oscilloscope to look for evidence of nonlinear absorption due to the pump beam. The laser power was always kept below the threshold for saturation of the detector.

The transient absorption (TA) spectra were numerically corrected for the chirp of the continuum, which corresponds to differences in arrival times of the different wavelength constituents due to self-phase modulation and group velocity dispersion primarily in the 1 cm thick cell of water. The chirp dynamics was determined by measuring the TA signal for various time delays in ZnSe; the signal is ostensibly due to an instantaneous two-photon absorption (TPA) when excited simultaneously by one photon each from the pump and probe beams. TPA from either beam alone was not possible since the peak intensity was orders of magnitude below the threshold ($\approx 10^{11}$ W/cm²) for generating free carriers.¹⁷ Moreover, the subpicosecond response at each probe wavelength indicated that such a process, which has a lifetime of more than a 1 ns in ZnSe,¹⁷ was not operative.

The spectrum of the absolute magnitude of the third-order optical nonlinear susceptibility $\chi^{(3)}(-3\omega; \omega, \omega, \omega)$ of $PtCl$ was measured with the output of an optical parametric generator/amplifier (OPG/OPA) comprising two beta barium borate (BBO) crystals cut for type-I phase matching, and aligned for single-pass pumping using the frequency tripled (355 nm) output from a mode-locked Nd:YAG laser (Continuum Model PY 61) with 35 ps pulsewidth and 6 mJ per pulse at 10 Hz repetition rate. The infrared output (idler beam) from the OPG/OPA constituted the fundamental beam in the third-harmonic generation (THG) experiment, and was focused onto the sample by a 5X microscope objective,¹⁸ whereas the visible output (signal beam) was used to monitor the pulse-to-pulse fluctuation of the laser. In spite of the tight focusing of the idler beam, we found no contribution to the third-harmonic signal from the air to which the sample was exposed. The sample was mounted on a rotational stage for generation of Maker fringes. At each wavelength, third-harmonic signals from the sample and from the fused silica substrate were measured in sequence. Assuming a value of $\chi^{(3)}(-3\omega; \omega, \omega, \omega)$ for fused silica of 3.1×10^{-14} esu,¹⁹ we calculated that for the sample according to¹⁹

$$\chi_s^{(3)}(-3\omega; \omega, \omega, \omega) = \chi_{ref}^{(3)} \sqrt{\frac{I_s}{I_{ref}}} \left(\frac{n_s}{n_{ref}} \right)^2 \frac{L_s}{L_{ref}} K_s; \quad (1)$$

$$K_s = \frac{\ln T_3 - 3 \ln T_1}{T_3/2 - (3/2)T_1}, \quad (2)$$

where I is the intensity of the third-harmonic signal obtained from fitting Maker fringes, n is the index of refraction, L is thickness, and the subscripts s and ref refer to the $PtCl$ sample and substrate, respectively. K_s is a correction factor for absorption (α_1 and α_2) of both the third-harmonic signal and incident fundamental beams, with transmission coefficients $T_1 = \exp(-\alpha_1 L_s)$ and $T_3 = \exp(-\alpha_2 L_s)$, respectively.

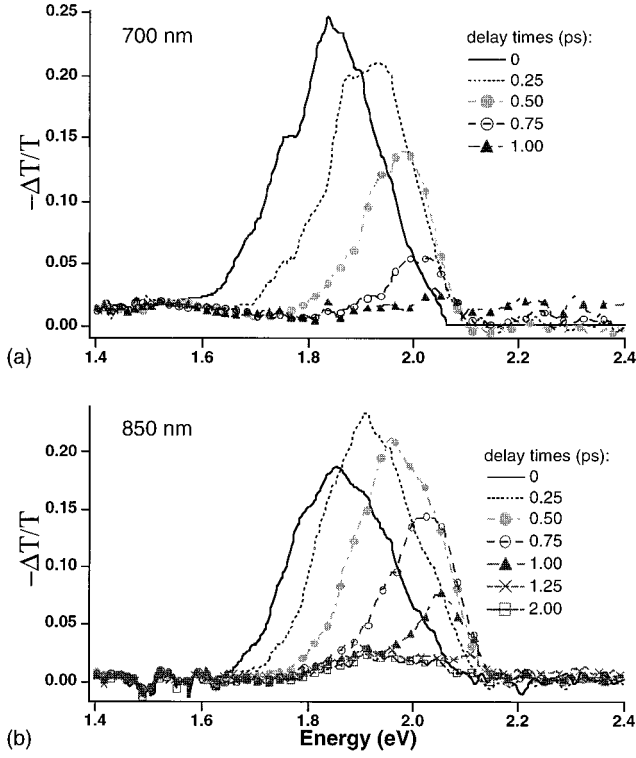


FIG. 2. Transient absorption spectra of PtCl for excitation at (a) 1.78 eV and (b) 1.46 eV.

We assume that the magnitude of $\chi^{(3)}(-3\omega; \omega, \omega, \omega)$ changes slightly according to Miller's rule in the wavelength range of 900 nm–1.8 μm . The corresponding energy range (0.8–1.2 eV) of the incident photons allowed us to fill a wide gap in the previously measured spectrum.¹⁰ All measurements were performed at 290 K with light beam polarizations parallel to the axis of the linear chains.

III. RESULTS AND DISCUSSION

A. Excitation regimes

1. Intrinsic polarons

Figure 2 shows the TA spectrum resulting from excitation energies well below the edge of the exciton. With $E_{\text{pump}} = 1.77$ eV (700 nm), a band initially appears at 1.80 eV (probe energy), blueshifts to above 2.1 eV within 1 ps [Fig. 3(a)], and then appears to completely decay [Fig. 4(a)] in 1.5 ps (the blueshift combined with the lack of transmission above 2.2 eV, however, obscure the dynamics for longer times). Similar results are observed as we decrease E_{pump} to 1.38 eV (900 nm). For $E_{\text{pump}} = 1.38$ and 1.46 eV (850 nm), however, an additional peak appears that does not shift in energy with time [Fig. 2(b)]. TA band blueshifts have been observed for other 1D materials, such as conducting polymers. In polydiacetylene, for example, a blueshift takes place within 0.5 ps and is attributed to the relaxation of the photoexcited exciton into a self-trapped state.²⁰ A similar blueshift is seen in polyacetylene,²¹ also within 0.5 ps, and associated with lattice relaxation around the photoinduced charged defect.

According to the linear absorption at 290 K,¹³ photons of energy below 2 eV cannot generate the lowest optical exci-

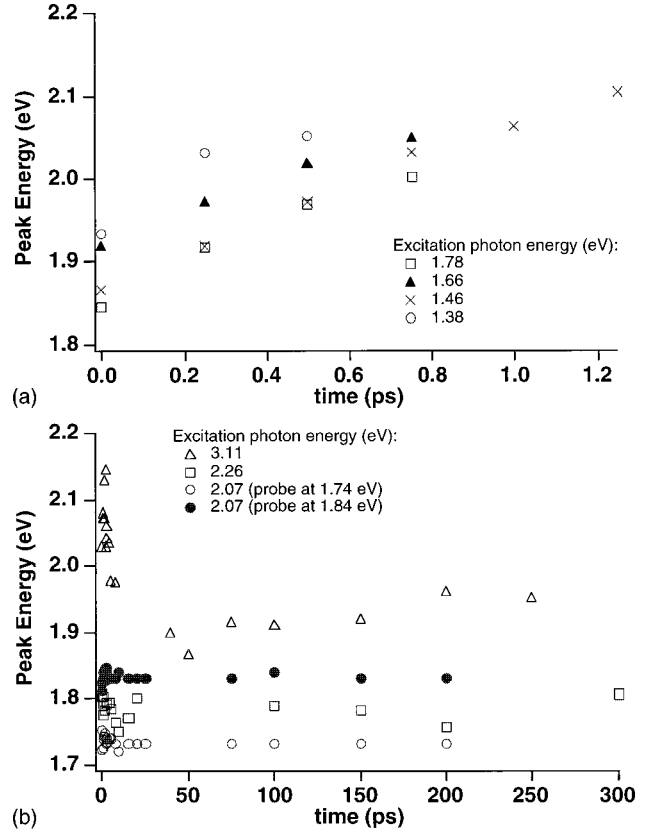


FIG. 3. Evolution of the peak energy of the transient absorption band for wavelengths from (a) 700 to 900 nm and (b) 400 to 600 nm.

ton. Therefore, the observed excitation must arise from either a phonon-assisted transition, multiphoton absorption, or absorption involving an intrinsic defect level. Phonon-assisted absorption is possible, but unlikely, since the vibration most likely coupled is the symmetric stretch ν_1 of the Cl atoms around the Pt⁴ sites, which has an energy E_p of only 0.038 eV.⁴ In a linear system, excitation at 1.38 eV would therefore require absorption of about 19 of these phonons, an event that has a negligibly small probability. Although higher frequency, off-chain vibrations could also be involved in this process, a large number of quanta would still be required.

We checked for two-photon absorption by measuring the intensity dependence of the transmission of the pump beam. Assuming rectangular spatial and temporal profiles for the pump, one expects the transmission to vary as

$$\frac{1}{T} = \frac{e^{\alpha d}}{(1-R)^2} \left[1 + \beta(1-R)I_0 \frac{(1-e^{-\alpha d})}{\alpha} \right], \quad (3)$$

where α and β are one and two-photon absorption coefficients, respectively, I_0 is the incident peak intensity, R is the reflectivity, and d is the sample thickness. A significant two-photon component to the excitation should therefore lead to a linear increase in $1/T$ with I_0 . In particular, one might expect to observe such a nonlinear dependence for $E_{\text{pump}} < 1.8$ eV since there is evidence for an even-parity state $|mg\rangle$ around 3.3 to 3.8 eV.^{8,10} However, as Fig. 5 shows, T is linear in pump intensity for all $E_{\text{pump}} \leq 2.3$ eV. (The large error bars at low light intensity are associated with the small voltage out-

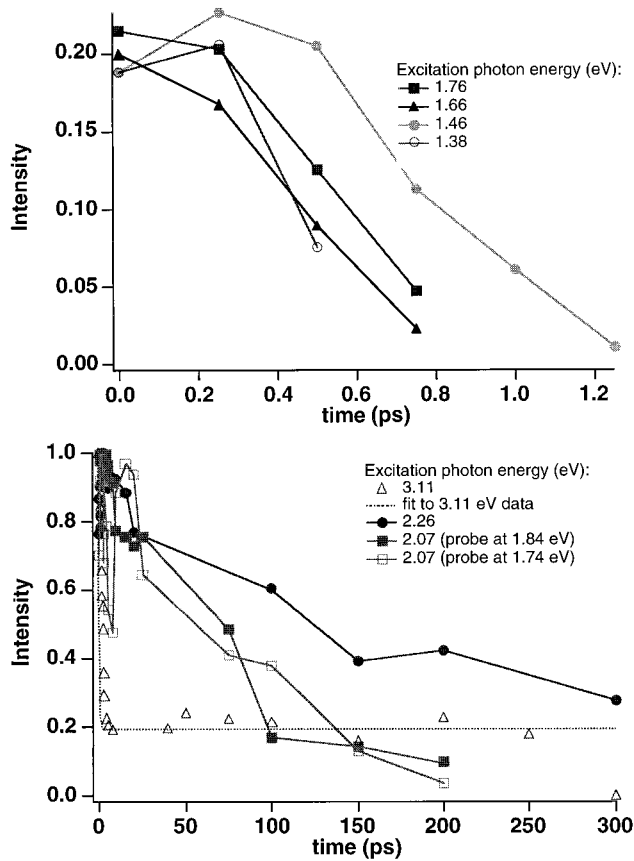


FIG. 4. Time dependence of the transient absorption signal for pump wavelengths from (a) 700 to 900 nm, and (b) from 400 to 600 nm. Solid lines are guides to the eye.

put of the photodiode relative to the sensitivity of the oscilloscope, and the dominance of scattered, rather than transmitted light, reaching the detector at these low light levels.) This is not surprising in view of the small pump intensities, corresponding to the narrow portions of the continuum, which we select but do not optically amplify.

Since we can rule out multiphonon and two-photon absorption in association with the pump photons, we conclude that excitation between 1.38 and 1.77 eV involves intrinsic defect levels, most likely the ones responsible for the *A* band in the linear absorption. In fact, this band is present in the optical density spectrum of each of our samples, although its intensity relative to the exciton band could not be quantified due to the large optical thicknesses of the samples, which prevented measurement of the exciton absorption beyond its tail. There is strong evidence that the *A* band is associated with polarons,²² the optical transition occurring between the two gap states. Resonance Raman studies²³ have shown that the *A* band is actually a composite of absorptions from both electron and hole polarons, which have different optical transition energies due to charge conjugation asymmetry in *MX* systems.¹⁵ Consequently, we expect there to be slightly different responses in the TA depending on whether P^- or P^+ is excited. We believe that such asymmetry may be responsible for the additional absorption band [Fig. 2(b)] appearing after 1 ps at 1.95 eV that decays in 2 ps when we pump into the P^- absorption band. Although we do not

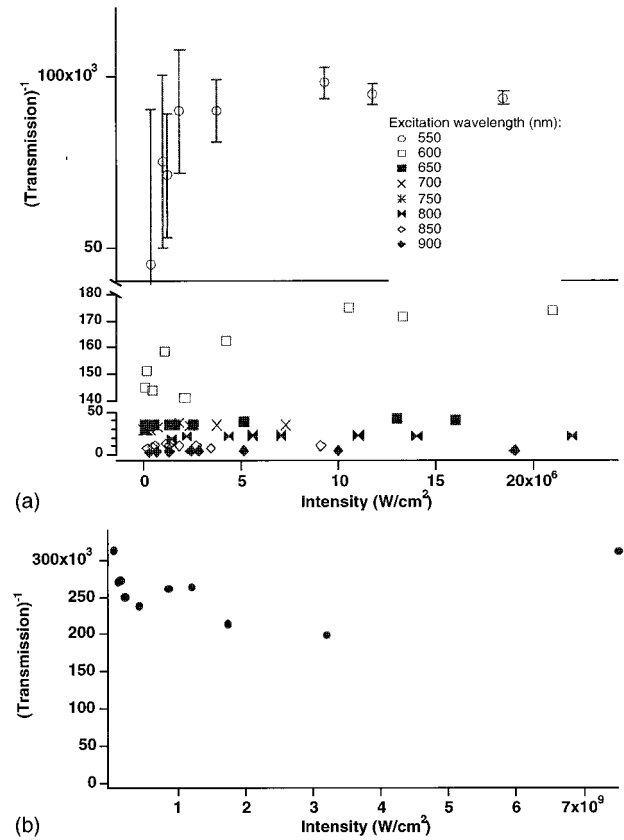


FIG. 5. Intensity dependence of transmission for wavelengths from (a) 550 to 900 nm and (b) 400 nm.

know the parity of the upper polaron state, the TA band energy (1.8–1.9 eV) at $t=0$ in Fig. 2, may be consistent with a transition to $|mg\rangle$.

The blueshift of the TA upon subgap excitation can then be understood in terms of lattice relaxation of the photoexcited polaron (Fig. 6). A change in the electron occupancy of

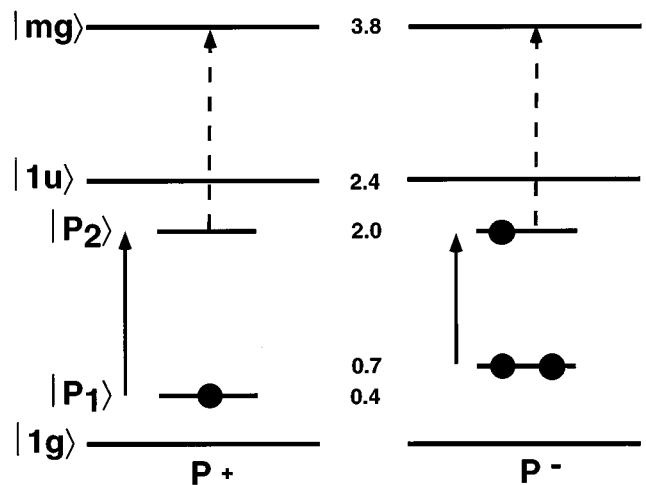


FIG. 6. Scenario for photoexcitation of pre-existing polarons in PtCl. The numbers represent the energies of the levels with respect to the ground state $|1g\rangle$. Solid and dashed lines with upward arrows are optical transitions induced by the pump and probe, respectively. The solid spheres are electrons occupying polaron levels P_1 and P_2 .

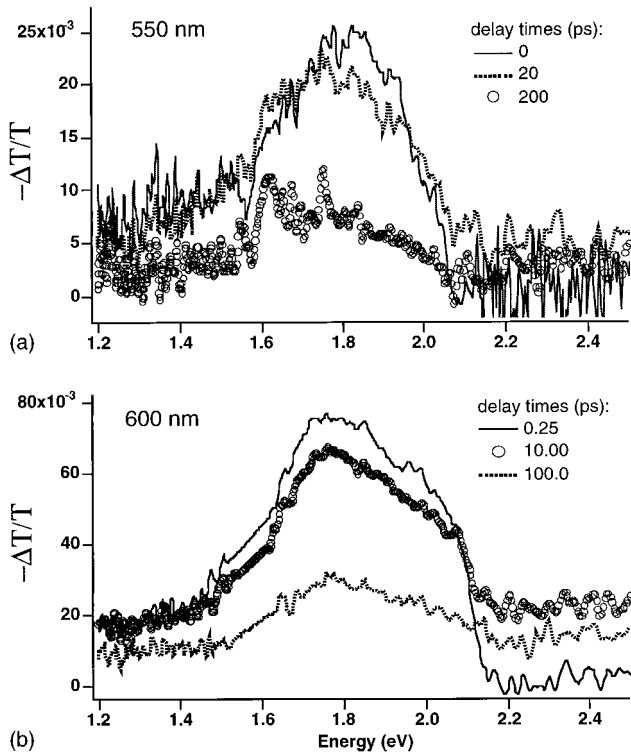


FIG. 7. Transient absorption spectra of PtCl for excitation at (a) 2.26 eV and (b) 2.07 eV.

the localized states, in general, and the promotion of an electron from the lower $|P_1\rangle$ to upper level $|P_2\rangle$, in particular, is predicted to lead to an evolution of the gap states toward the gap center, concomitant with structural relaxation.⁶ As this happens, the probe transition energy from $|P_2\rangle$ to $|mg\rangle$ increases. We assume that this level is at 2.0 eV above the ground state $|1g\rangle$ for both P^+ and P^- . This is based on the experimentally observed A band transition energy in the steady state of ≈ 1.3 eV for P^- , and 1.6 eV for P^+ , and an energy difference between $|1g\rangle$ and the lower P^+ level, or between $|1u\rangle$ and the upper P^- level, of about 0.4 eV.²⁴

2. Exciton tail states

Excitation into the exciton absorption tail leads to the TA spectra of Fig. 7; Fig. 7(a) shows the TA for pump energy $E_{\text{pump}}=2.26$ eV (550 nm). Within the experimental time resolution a subgap band is formed that can be reasonably fit to a Gaussian at 1.80 eV that decays [Fig. 4(b)] with an exponential time constant of 210 ps. This is close to the relaxation time of 230 ps of the photoluminescence (PL) induced by 2.31 eV excitation and detected between 1.3 and 1.5 eV.²⁵ The TA spectrum [Fig. 7(b)] for $E_{\text{pump}}=2.07$ (600 nm) is similar in shape to the one formed upon 2.26 eV excitation, but, with the improved signal-to-noise ratio in this spectrum, is more obviously comprised of two bands, which are centered at 1.74 and 1.84 eV. The latter has an exponential time constant $\tau=80\pm 10$ ps; the scatter in the data for the other peak at short times complicates the fit, but the time constant is approximately the same. This relaxation time is in good agreement with that (100 ± 30 ps) found for the PL decay in PtCl for 2.13 eV excitation.²⁶

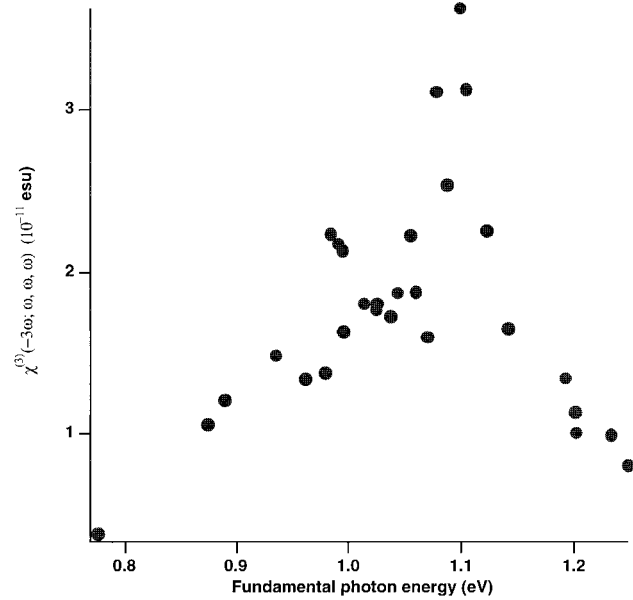


FIG. 8. Spectrum of the absolute magnitude of $\chi^{(3)}$.

The observed dependence of relaxation rate on excitation wavelength for $E_{\text{pump}}>2$ eV is opposite that of structurally inhomogeneous 1D systems. In a disordered form of PtCl,²⁵ as well as in PPV,¹³ the PL decay rate increases with both excitation energy and detection energy within the tail of the exciton absorption, and is attributed to an exciton hopping rate that is proportional to the density of states to which the exciton can hop. In our measurements, the decay rate decreases as we increase E_{pump} within the tail. The PL results of Tanino, Rühle, and Takahashi,²⁶ on PtCl also show a decreased decay rate with detection energy. Although it has been suggested that this behavior is associated with defects,²⁵ both the PL (Ref. 26) and the present TA dynamics can be fit by simple exponential decays, indicative of an ordered system. In addition, for excitation above the exciton band edge, relaxation mediated by multiple trapping in localized states has been shown for 3D semiconductors to lead to a blueshift of the TA spectrum with time,²⁷ which is not observed for PtCl [Fig. 3(b)].

The transient PL in PtCl around 1.8 eV has been attributed^{11,25,26} to the lowest odd-parity exciton, which is predicted to become quickly self-trapped by its strong interaction with the lattice in 1D systems. Another possibility is that we are primarily populating an even-parity state $|2g\rangle$ that lies at an energy lower than $|1u\rangle$. The dipole-forbidden transition from $|2g\rangle$ to $|1g\rangle$ would then explain the weakness of the PL intensity (2.5% quantum efficiency).²⁶ We conjecture that $|2g\rangle$ is populated by internal conversion from $|1u\rangle$ in a time that is beyond our resolution (less than 300 fs). Such a rapid transition has been observed in molecular analogs of polyacetylene: In excited carotenoids, energy transfer to chlorophylls occurs through the decay of the lowest one-photon allowed excited singlet into an optically forbidden state below it within 200 fs.²⁸ Consequently, we assign the high-energy edge of the PL in PtCl at 1.45 eV to $|2g\rangle$.²⁵ Figure 8 shows the THG spectrum, which we can use to determine the energies of other excited states. In particular, we observe a prominent band for a single photon at 1.1

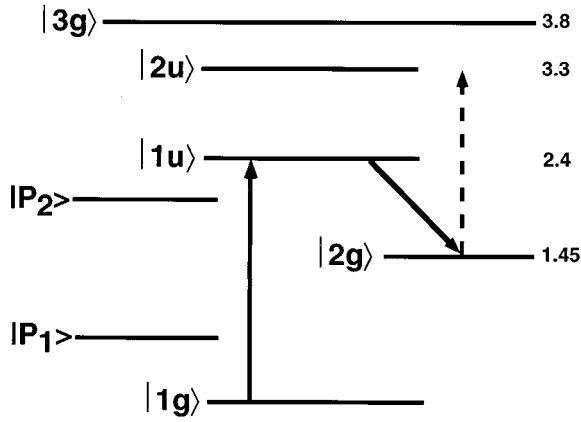


FIG. 9. Scenario for photoexcitation of excitons in PtCl. The numbers represent the energies of the levels with respect to the ground state. Solid and dashed lines with arrows pointing toward the top of the page are transitions induced by the pump and probe, respectively. The line with the downward pointing arrow represents internal conversion from $|1u\rangle$ to $|2g\rangle$.

eV, that could arise from two- or three-photon resonances, or even a resonance associated with the difference in energy between excited states.²⁹ However, a three-photon resonance from $|1g\rangle$ corresponds well with a band that peaks at 3.5 eV in the linear absorption.¹⁴ In addition, assuming excitation into $|2g\rangle$, the existence of an odd-parity state ($|2u\rangle$) at 3.3 eV would explain why we observe a TA band at 1.85 eV (Fig. 7), for both 550 and 600 nm excitations. Unfortunately, it has not been possible to verify the existence of $|1u\rangle$ around 2.4 eV through THG spectroscopy since there is a gap in the fundamental energy photons that could be produced this spectral range.

The origin of the lower energy transition at 1.74 eV [Fig. 7(b)] in the TA for $E_{\text{pump}}=2.07$ eV is still not clear, but is probably related to $|2g\rangle$ because their dynamics are similar to each other. However, the small difference in the TA spectrum and the faster relaxation for this excitation energy compared to the case for $E_{\text{pump}}=2.26$ eV, is tentatively attributed to correspondingly different distributions of vibrationally excited states created within the $|1u\rangle$ potential surface.

Although competition between the $|2g\rangle$ and relaxed $|1u\rangle$ leads to a reduced efficiency of PL from the odd-parity state, we do not see distinct bands in the TA spectrum with different dynamics from each other. Since the relaxation appears instead to be uniform across the spectrum, we believe the PL is almost entirely from $|2g\rangle$. In addition, impurities and interchain interactions can lead to a mixing of even and odd states, causing the lowest excitonic state to have an odd-parity component, and increasing the PL efficiency from that level. Figure 9 shows an energy-level diagram for the process of exciton formation ignoring such mixing. An electron is initially pumped from $|1g\rangle$ into $|1u\rangle$. However, as a result of structural relaxation the exciton quickly becomes localized and relaxes into $|2g\rangle$. This can be simply modeled by the rate equation,

$$\frac{dn_1}{dt} = n_0 W_{\text{pu}} - n_1 \nu_{\text{PL}}, \quad (4)$$

where n_0 is the electron density in the ground state, and n_1 that in $|2g\rangle$, W_{pu} is the pump rate, and ν_{PL} is the rate of relaxation out of n_1 , which has been determined from transient PL. We assume in Eq. (4) that relaxation from $|1u\rangle$ to $|2g\rangle$ occurs within the width τ of the pump pulse. If N is the initial population of the ground state, we have

$$n_1(t) = N e^{-\nu_{\text{PL}} t} \int_0^t dt' W_{\text{pu}}(t') e^{\nu_{\text{PL}} t'}, \quad (5)$$

where we have assumed that excited populations are small compared to n_0 , which therefore remains relatively constant. The change in absorption associated with transitions from $|2g\rangle$ is then

$$\Delta\alpha \sim \int_{-\infty}^{+\infty} dt' n_1(t') I_{\text{pr}}(t-t'), \quad (6)$$

where I_{pr} is the intensity of the probe pulse. For a square pump pulse with $\tau \ll 1/\nu_{\text{PL}}$, which is satisfied in our experiment since $\tau \approx 0.3$ ps and $1/\nu_{\text{PL}} \approx 10^2$ ps, Eq. (5) gives $n_1 \sim \exp(-\nu_{\text{PL}} t)$. Since the probe pulse is also short with respect to the lifetime of $|2g\rangle$, the TA [Eq. (6)] will apparently have the same time dependence as the PL, which is what we observe.

A puzzling aspect of the data is the apparent lack of bleaching in the TA spectra. For exciton formation (Fig. 7), however, the bleaching is presumably in the high-energy region in which light polarized parallel to the chains is completely absorbed. In addition, bleaching of small magnitude would probably be obscured by the TA that is perpendicularly polarized. For excitation of pre-existing polarons (Fig. 2) we expect some bleaching to appear at the energy of the defect band in the ground state absorption. However, given the larger density of states in the bands, particularly at their edges, where there is a singularity in 1D, most of the oscillator strength for the transitions associated with this new state would come from the exciton band, which, as above, is beyond our spectral range. In addition, the spatial localization of the polaron may give rise to a bleaching band that is so broad, that its intensity is below our detection limit. The blueshift in the TA band shows that the polaron becomes more localized upon photoexcitation since the levels associated with it move deeper into the gap. Thus, the bleaching would be even more spread out after photoexcitation.

3. Excitons and polarons

For $E_{\text{pump}}=3.1$ eV (400 nm) (Fig. 10), which is well above $|1u\rangle$, a TA band appears around 2.0 eV, with a decay (solid line is a biexponential fit) that is initially faster (1.75 ps) than for the excitations of Fig. 7, followed by a slow response with a time constant of 750 ps. The fast component appears to be associated with a small blueshift of the spectrum [Fig. 3(b)], indicative of an optical transition originating from a level that shifts downward in energy during relaxation, and is similar to what was observed [Fig. 3(a)] for photoexcitation of intrinsic polarons. For this higher excitation energy, however, we ostensibly generate polarons that did not exist in the dark.⁶ The propensity for generating charge carriers for E_{pump} above the $|1u\rangle$ exciton band edge has recently been demonstrated for a wide variety of *MX*

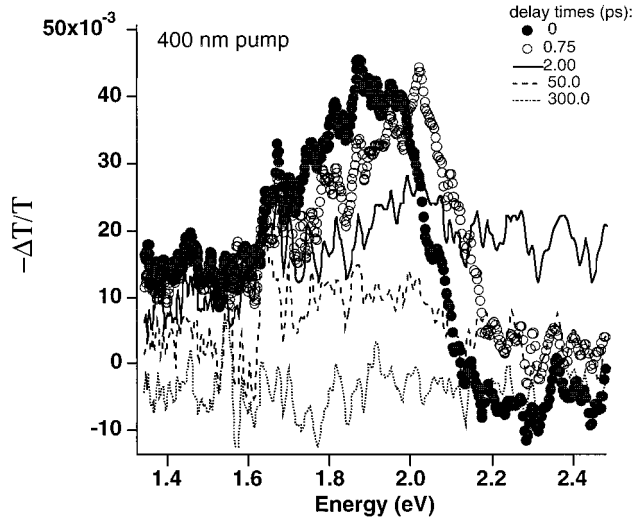


FIG. 10. Transient absorption spectra of PtCl for excitation at 3.1 eV.

systems in CW TA and PL experiments.³⁰ In PtCl this may occur via phonon-assisted excitation into $|2u\rangle$ (at 3.3 eV). Then if the electron-hole separation r_0 in this state is large, free carriers may be immediately generated, but quickly evolve into polarons due to the 1D nature of the system. The $2u$ state may therefore be analogous to the nBu conduction band in conducting polymers, which also has a large three-photon resonance in THG above that for the $1Bu$ exciton.³¹

A slower process of polaron formation would involve generation of a $|1u\rangle$ exciton with enough excess energy to allow dissociation into isolated polarons.¹⁶ The redshift [Fig. 3(b)] of the TA spectrum that is observed after 2 ps, but which lasts about 50 ps, could then be correlated with a transition from $|P_1\rangle$, which shifts in a direction opposite that of $|P_2\rangle$.⁶ Assuming final densities of states that were roughly equal to each other, one would expect, under photogeneration of polarons, the transition probability from P_1 to be greater than that from P_2 since P_1 is either singly or doubly occupied, whereas P_2 has either zero or only one electron. This may explain the dominance of the redshift at long times, but not the initial blueshift.

Excitons that do not dissociate may be responsible for the remaining signal that has a 750 ps decay time constant, which is much greater than the relaxation rate for tail-state excitation [Figs. 4(b), 7]. The origin of the dependence of relaxation rate on E_{pump} could then lie in the differences in the phonon spectra generated in the excited state in each case. For example, as the excess energy increases, the fraction of high-order vibrational modes may increase, leading to lower transition probabilities, and, therefore, slower decays. It could also be argued, in contrast to the density of states model, that exciting deeper into the exciton band increases the electron-hole kinetic energies, causing r_0 to increase, and therefore leading to an increased recombination time due to tunneling, assuming that r_0 is smaller than the Coulomb capture radius. This phenomenon has been used to explain the kinetics of TA in 3D amorphous semiconductors as a function of E_{pump} .³²

B. Intrachain vs interchain interactions

Theoretical studies have shown that the presence of localized nonlinear lattice excitations known as breathers causes

the energies of the intragap and band edge levels to oscillate with a period equal to the LO phonon lifetime (≈ 250 fs for PtCl).⁶ This oscillation is suppressed by adding a damping term to the equation of motion of the ions along the chain to suppress the formation of breathers.³³ The damping represents alternative pathways for relaxation, such as 3D interactions, and may explain why we do not observe an oscillation of the TA band energy. The role of interchain interactions in quasi-1D systems has received much attention since it was recently determined, by subpicosecond absorption measurements, that interchain excitons may actually be the primary photoexcitations in films of the conjugated polymer PPV.³⁴ The importance of such interactions—between the chain and the ligands and counterions—in MX systems has also been demonstrated recently through x-ray crystallography and resonance Raman measurements.¹

Evidence for higher-dimensional interactions in the present data is a feature in the TA spectra that appears only for $E_{\text{pump}} > 1.9$ eV. It has a relatively flat absorption profile for probe energies above 2.1 and below 1.4 eV [Figs. 7 and 10, and also seen for $E_{\text{pump}} = 1.91$ eV (not shown)] that displays the same relaxation dynamics as the prominent bands, but has an onset that is delayed by 0.5–1.0 ps with respect to the pump pulse. Since light polarized parallel to the chains is not transmitted for the high-energy region in which this feature appears, we attribute it to a portion of the white-light continuum that is polarized perpendicular to the chains. This is caused by probe light that leaks through the polarizer perpendicular to its axis of easy transmission. The origin of this off-chain absorption is either an induced transition dipole moment that has a perpendicular component, or an interchain excitation, such as an exciton bound across adjacent chains. We rule out the latter because the dominant excited-state species for pump polarization parallel to the chains should be the intrachain exciton consisting of neighboring Pt^{3+} sites, and we expect the relaxation of such a state to be much faster than that of an interchain excitation. However, the large oscillator strength of this transition and its dynamics, identical to that of the main TA band, suggest that it originates from the same electronic state. An alternative mechanism for this absorption is that the excess energy of the pump beyond that used to create the exciton is channeled into large-amplitude out-of-chain vibrations, leading to the formation of a 2D or 3D structural kink in the chain. In conjugated polymers and their analogous finite polyenes, for instance, photoexcitation is postulated to generate structural distortions involving out-of-plane twists of the carbon backbone, with an associated electronic state below the lowest optically allowed excited state.³⁵ In MX systems, energy dissipation via off-chain modes, like those of the (en) ligands or the ClO_4^- counterions, is probably favored, since these have much higher frequencies (1113 and 935 cm^{-1} for the symmetric stretches, respectively)^{36,37} than the intrachain modes, which are confined to frequencies less than or equal to that of ν_1 at 311 cm^{-1} ,^{4,38} and, consequently, would require fewer vibrational quanta for relaxation.

IV. SUMMARY AND CONCLUSIONS

A summary of the TA data is provided in Table I. We observe a dramatic change in the spectrum and in the dynam-

TABLE I. Excited-state properties of PtCl. Assignments, based on Figs. 6 and 9, are given to the optical transitions associated with the pump and probe photons. The range of transient absorption peak energies for pump photons of 1.38 to 1.78 eV, and for 3.10 eV, results from transient shifts of the peaks.

Pump photon energy (eV)	Optical transition of pump	Optical transition of probe	Transient absorption peak (eV)	Lifetime (ps)
3.10	$1g \rightarrow 1u, 1g \rightarrow 2u$	$P_2 \rightarrow 3g, 2g \rightarrow 2u$	1.9–2.1	1.75, 750
2.26	$1g \rightarrow 1u$	$2g \rightarrow 2u$	1.8	230
2.07	$1g \rightarrow 1u$	$2g \rightarrow 2u$	1.74, 1.84	80
1.78	$P^+ : (P_1 \rightarrow P_2)$	$P_2 \rightarrow 3g$	1.8–2.1	<1
1.66	$P^+ : (P_1 \rightarrow P_2)$	$P_2 \rightarrow 3g$	1.8–2.1	<1
1.46	$P^- : (P_1 \rightarrow P_2)$	$P_2 \rightarrow 3g$	1.8–2.1	<1
1.38	$P^- : (P_1 \rightarrow P_2)$	$P_2 \rightarrow 3g$	1.8–2.1	<1

ics of photoexcited states of PtCl as we tune the excitation wavelength across the edge of the lowest optical exciton $|1u\rangle$. For E_{pump} well below $|1u\rangle$, but in resonance with the A band in the linear absorption, we found that we could photoexcite pre-existing polarons with high quantum efficiency. The resulting species appears to decay within about 1 ps. Upon pumping into the tail of the lowest odd-parity exciton band, a transient absorption signal appears that displays the same relaxation dynamics as photoluminescence, with an excited-state lifetime on the order of 10^2 ps. We believe this signal originates from an even-parity state $|2g\rangle$ that is populated by internal conversion from the initial exciton. For higher excitation photon energies, we suspect that we generate both excitons and polarons, the latter being created either as free carriers through phonon-assisted absorption into a continuum, or through dissociation of the $1u$ exciton. The excitons that do not dissociate decay into $|2g\rangle$, giving rise to a slowly decaying component to the TA and to an off-chain absorption. Interactions perpendicular to the chain will allow

for additional pathways for energy dissipation that compete with breathers, which may be quenched when other relaxation mechanisms are important.

ACKNOWLEDGMENTS

We thank A. R. Bishop, J. Tinka Gammel, and A. B. Saxena for valuable discussions, D. McBranch and V. Klimey for helping with the initial transient absorption setup, A. P. Shreve for his expertise with the optical amplifier, and S. R. Johnson for synthesizing the PtCl crystals. This work was funded by the Division of Materials Science of the Office of Basic Energy Sciences of the United States Department of Energy (DOE). The work performed at Sandia National Laboratories was supported by the DOE under Contract No. DE-ACO4-94AL85000. Sandia is a multiprogram laboratory operated by Sandia Corporation, a Lockheed Martin Company, for the DOE.

- ¹B. Scott, S. P. Love, G. S. Kanner, S. R. Johnson, M. P. Wilkerson, M. Berkey, B. I. Swanson, A. Saxena, X. Z. Huang, and A. R. Bishop, *J. Mol. Struct.* **356**, 207 (1995).
- ²D. Baeriswyl and A. R. Bishop, *Phys. Scr.* **T19**, 239 (1987); J. Tinka Gammel, I. Batistic, A. R. Bishop, E. Y. Loh, Jr., and S. Marianer, *Physica B* **163**, 458 (1990).
- ³G. S. Kanner, J. Tinka Gammel, S. P. Love, S. R. Johnson, B. Scott, and B. I. Swanson, *Phys. Rev. B* **50**, 18 682 (1994).
- ⁴F. H. Long, S. P. Love, B. I. Swanson, and R. H. McKenzie, *Phys. Rev. Lett.* **71**, 762 (1993).
- ⁵A. J. Heeger, S. Kivelson, J. R. Schrieffer, and W.-P. Su, *Rev. Mod. Phys.* **60**, 781 (1988).
- ⁶J. Tinka Gammel, A. Saxena, I. Batistic, A. R. Bishop, and S. R. Phillpot, *Phys. Rev. B* **45**, 6408 (1992).
- ⁷R. Kersting *et al.*, *Mol. Cryst. Liq. Cryst.* **256**, 9 (1994); H. Bässler *et al.*, *Synth. Met.* **49**, 341 (1992).
- ⁸Y. Wada and M. Yamashita, *Phys. Rev. B* **42**, 7398 (1990), and references therein.
- ⁹Z. Shuai, D. Beljonne, J. L. Brédas, A. Saxena, and A. R. Bishop, *Solid State Commun.* **97**, 1063 (1996).
- ¹⁰Y. Iwasa, E. Funatsu, T. Koda, M. Yamashita, H. Kobayashi, and K. Kubodera, *Mol. Cryst. Liq. Cryst.* **217**, 37 (1992).
- ¹¹R. I. Donohoe, L. A. Worl, C. A. Arrington, A. Bulou, and B. I. Swanson, *Phys. Rev. B* **45**, 13 185 (1992); H. Okamoto, T. Mitani, K. Toriumi, and M. Yamashita, *Phys. Rev. Lett.* **69**, 2248 (1992); H. Okamoto *et al.*, *Mol. Cryst. Liq. Cryst.* **256**, 161 (1994).
- ¹²H. Ooi, M. Yamashita, and T. Kobayashi, *Solid State Commun.* **86**, 789 (1993); H. Ooi, M. Yoshizawa, M. Yamashita, and T. Kobayashi, *Chem. Phys. Lett.* **210**, 384 (1993).
- ¹³R. Kersting *et al.*, *Phys. Rev. Lett.* **70**, 3820 (1993).
- ¹⁴M. Tanaka, S. Kurita, T. Kojima, and Y. Yamada, *Chem. Phys.* **91**, 257 (1984).
- ¹⁵J. Tinka Gammel, R. J. Donohoe, A. R. Bishop, and B. I. Swanson, *Phys. Rev. B* **42**, 10 566 (1990).
- ¹⁶S. Kurita, M. Haruki, and K. Miyagawa, *J. Phys. Soc. Jpn.* **57**, 1789 (1988).
- ¹⁷J. A. Bolger *et al.*, *Opt. Commun.* **97**, 203 (1993).
- ¹⁸F. Kajzar and J. Messier, *Phys. Rev. A* **32**, 2352 (1985).
- ¹⁹M. Thallhammer and A. Penzkofer, *Appl. Phys. B* **32**, 137 (1983).
- ²⁰M. Yoshizawa, Y. Hattori, and T. Kobayashi, *Phys. Rev. B* **49**, 13 259 (1994).

- ²¹L. Rothberg, T. M. Jedju, P. D. Townsend, S. Etemad, and G. L. Baker, *Phys. Rev. Lett.* **65**, 100 (1990).
- ²²S. Kurita and M. Haruki, *Synth. Met.* **29**, F129 (1989).
- ²³R. J. Donohoe, C. D. Tait, and B. I. Swanson, *Chem. Mater.* **2**, 315 (1990).
- ²⁴R. J. Donohoe, S. A. Ekberg, C. D. Tait, and B. I. Swanson, *Solid State Commun.* **71**, 49 (1989).
- ²⁵Y. Wada, U. Lemmer, E. O. Göbel, M. Yamashita, and K. Toriumi, *Phys. Rev. B* **52**, 8276 (1995).
- ²⁶H. Tanino, W. W. Rühle, and K. Takahashi, *Phys. Rev. B* **38**, 12 716 (1988).
- ²⁷J. Orenstein and M. A. Kastner, *Solid State Commun.* **40**, 85 (1981).
- ²⁸R. J. Cogdell, T. Gillbro, O. O. Andersson, R. S. H. Liu, and A. E. Asato, *Pure Appl. Chem.* **66**, 1041 (1994).
- ²⁹N. Bloembergen, H. Lotem, and R. T. Lynch, Jr., *Indian J. Pure Appl. Phys.* **16**, 151 (1978).
- ³⁰Y. Wada, N. Matsushita, J. Tanaka, and T. Mitsuhashi, *J. Lumin.* **66**, 120 (1996); H. Okamoto *et al.*, *Synth. Met.* (to be published).
- ³¹D. Guo *et al.*, *Phys. Rev. B* **48**, 1433 (1993); S. Abe, M. Schreiber, W. P. Su, and J. Yu, *ibid.* **45**, 9432 (1992).
- ³²Z. Vardeny and J. Tauc, in *Semiconductors Probed by Ultrafast Laser Spectroscopy*, edited by R. Alfano (Academic, New York, 1984), p. 23.
- ³³A. B. Saxena (unpublished).
- ³⁴M. Yan, L. J. Rothberg, E. W. Kwock, and T. M. Miller, *Phys. Rev. Lett.* **75**, 1992 (1995).
- ³⁵B. I. Greene, J. Orenstein, R. R. Millard, and L. R. Williams, *Chem. Phys. Lett.* **139**, 381 (1987).
- ³⁶J. R. Campbell, R. J. H. Clark, and P. C. Turtle, *Inorg. Chem.* **17**, 3622 (1978).
- ³⁷G. Herzberg, *Molecular Spectra and Molecular Structure II. Infrared and Raman Spectra of Polyatomic Molecules* (Van Nostrand, Princeton, NJ, 1966).
- ³⁸S. P. Love *et al.*, *Phys. Rev. B* **47**, 11 107 (1993).